Indian Journal of Chemistry
Vol. 59A, September 2020, pp. 1259-1264

Degradation of Orange G and Malachite green dyes under visible light irradiation: Double layered core-shell nanoparticle as an efficient photocatalyst

Suganya Josephine GA[a] & Sivasamy A[b]*

[a]Department of Chemistry, Aarupadai Veedu Institute of Technology – Vinayaka Mission Research Foundation, Rajiv Gandhi Salai, Paiyanoor, Kancheepuram-603 104, Tamil Nadu, India
[a]Chemical Engineering Area, CSIR-Central Leather Research Institute, Adyar, Chennai-600 020, Tamil Nadu, India

*E-mail: arumugamsivasamy@yahoo.co.in

Received 14 April 2020; *accepted 28 July 2020*

Core-shell nanomaterials have emerged as a frontier area of focus in materials chemistry and catalysis. Here, we have explored the photocatalyst potential of a double layered core-shell material comprising a rare earth material as core and silica, zinc oxide as the subsequent shell materials. The prepared core-shell has average particle size of 40-60 nm, and the material has been characterized by FTIR, XRD, UV-DRS and FESEM techniques. The band gap energy of prepared material is 2.82 eV. The photocatalytic activity has been tested against Orange-G and Malachite green dye under visible light irradiation. A comparison for degradation of azo and non-azo dye has been elucidated. Preliminary studies with varying pH, catalyst dosage and initial dye concentration have been done to determine the optimum parameters for photocatalytic activity. The kinetic studies follow pseudo-first-order pathway. The prepared core-shell nanomaterial is found efficient for degradation of non-azo dye compared to azo dye. Both the materials show better activity than pristine ZnO. The photocatalyst is found to be environmentally benign with reusability even up to the third cycle of reuse.

Keywords: Environmental remediation, Malachite Green, Orange G, Photocatalysis, Visible light

Photocatalysis employing semiconductors nanomaterials are widely studied for degradation of organics from aqueous phase in synthetic organic chemistry for oxidation reduction reactions, in water splitting, as sensors, solar cells, etc.[1-6]. Semiconductor nano-materials *viz*. TiO_2, ZnO, Bi_2O_3, SnO_2 and WO_3 are widely studied for their photocatalytic and also anti-microbial applications[7-11]. Not only pristine semiconductor nanomaterials, but surface modification of the metal oxides by few techniques would also result in materials with enhanced photocatalytic properties. Surface modifications are often done by the process of doping metals, non-metals or rare earth materials onto the pristine metal oxide or by preparation of composites, core-shell, etc.[9,10]. Compared to other metal oxides, modified ZnO nanomaterials have a number of merits such as cost effectiveness and similar band gap energies compared to TiO_2. Various reports on doped ZnO recommend this to be a better semiconductor nanomaterial[11].

Dyes are a serious threat to humanity due to its widespread presence in the outlets from industries such as textile, leather, apparels, pharmaceuticals, etc.[12]. Different types of dyes are manufactured annually[13,14] out of which 10-25% of dyes are lost during the dyeing process[15]. The dye containing effluents are hazardous, non-biodegradable, carcinogenic or mutagenic to life forms, non-pleasing attire to the water (less than 1 ppm is also coloured) and stinking which has adverse effects on humans[16]. Orange G (OG) dye is an acid and mono-azo dye[17] employed as a colouring agent. Malachite green (MG) is a triphenylmethane toxic non-azo dye dye mostly used in aquaculture. Clemmenson *et al*. had studied the cytotoxicity of MG dye on Wistar rats and reported the LD_{50} to be 275 mg/kg[18]. Environmental monitoring agencies have made stringent guidelines for processing and made treatment of such contaminated effluents mandatory before released into the environment.

Recently, our group synthesized a two layered core-shell material containing a rare earth oxide, silica and zinc oxide by a template mediated synthesis[19]. The prepared nanomaterial showed considerable photocatalytic activity for degradation of 2,4-D, an endocrine disruptor under visible light irradiations. Since, the material possesses better capability for

degradation of endocrine disruptors, it is open for exploration of dye degradation efficiency for azo and non-azo compounds. As such, the material would be highly useful for the treatment of contaminated water containing any type of organics. In this study, we are reporting a double layered core-shell nanomaterials (DLCS) as a photocatalyst for degradation of OG and MG dyes under visible Light irradiation. We compared the azo and non-azo compound, and also did a complete kinetics study and by-product analysis.

Materials and Methods

Materials

Zinc nitrate hexahydrate (98%, $Zn(NO_3)_2{\cdot}6H_2O$), Tetraethyl ortho silicate (99. 9%, TeOS), zinc acetate tetrahydrate (99%, $Zn(OAC)_2{\cdot}4H_2O$) and dysprosium nitrate (99.9%, $Dy(NO_3){\cdot}6H_2O$), OG and MG dyes, were purchased from Sigma-Aldrich, India. Sodium carbonate, silver sulphate and sodium hydroxide were supplied by Sisco Research Laboratories, Mumbai, India. Cetyl trimethyl ammonium bromide (CTAB), ethanol, hydrochloric acid were purchased from Merck, Mumbai, India. All the chemicals were used as such without further purification.

Preparation of DLCS

DLCS was prepared by a three-step template mediated process as reported elsewhere[19]. In a typical procedure, the core layer of Dy_2O_3 was synthesized by a precipitation procedure wherein, an equimolar ratio of $Dy(NO_3){\cdot}6H_2O$ and Na_2CO_3 were prepared in double distilled (DD) water. To a stirred solution of $Dy(NO_3){\cdot}6H_2O$, Na_2CO_3 was added slowly and the resulting white precipitate was stirred further for 15 min and then filtered, washed with water and ethanol, dried and calcined at 700°C for 2 h. The resulting dysprosium oxide (DO) was ground and stored.

A solution of ethanol (250 mL), water (60 mL), ammonia (10.2 mL) and TEOS (1.2 mL) were stirred for 10 min at 40°C. To the above solution DO (1.0 g) and CTAB (0.6 g) were added and stirred at 40°C for 12 h. Then the solid was centrifuged, washed with hot water and dried and labelled as dysprosium oxide@silica (DS). DS (0.4 g) was taken and dispersed by sonication and then required amount of $Zn(OAC)_2{\cdot}4H_2O$ was added and precipitated by an equimolar solution of ammonium carbonate. The precipitates were stirred further for 15 min, filtered, washed, dried and calcined at 300°C for 3 h. Different ratio of core-shell DS:ZnO was prepared 1:1, 1:2, 1:2, and 1:4 and named as DLCS1, DLCS2, DLCS3 and DLCS4.

Photocatalytic studies

The photocatalytic studies for the degradation of OG and MG were conducted in a photoreactor (Annular Type, HEBER Scientific) capable of emitting light in the visible wavelength. A 500 W tungsten filament lamp was employed. The lamp was surrounded by an outer water jacket to remove the heat generated, and cooling fans were provided. The preliminary studies were performed in 10 mL volume of sample (6 h for OG and 1 h for MG) and kinetic studies in a 200 mL batch.

Results and Discussion

Characterization of DLCS

FTIR and XRD

The FTIR spectrum of DLCS photocatalysis is shown in Fig. 1A. The presence of R–O (Dy-O) and M–O (Zn-O) stretching vibrations were observed at 557 and 470 cm^{-1}, respectively. The Si-O stretching bands were observed at 800 and 1094 cm^{-1} respectively. A broad peak was also observed at

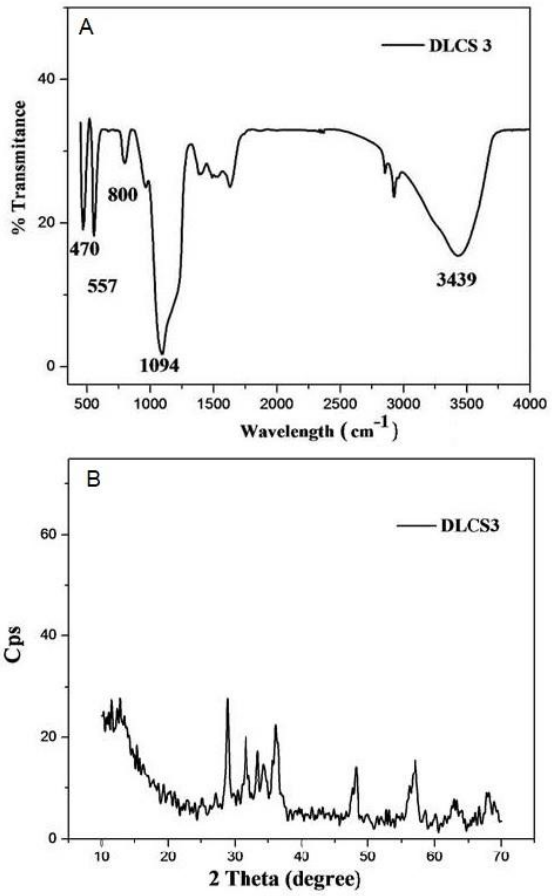

Fig. 1 — (A) FTIR spectrum and (B) XRD pattern of the prepared DLCS nanomaterial

3400 cm^{-1} which indicated the vibration of the surface adsorbed hydroxyl groups. These results potray that both zinc, silica and dysprosium were present as oxides in the prepared catalyst. In addition to these, few peaks were observed at 1200-1800 cm^{-1} which were probably due to the absorption of atmospheric CO_2 by the catalyst. The results were compared with literature[20-22]. Fig. 1B shows the XRD patterns of the prepared DLCS nanomaterial. The prepared core shell nanomaterial was found to be crystalline and the patterns were observed at (211), (222), (400), (440), and (622) which corresponds to Dy_2O_3 and (100), (002), (101), (102), (110), (103), (004), (112), and (201) are due to ZnO. The diffraction peaks were compared with the standard patterns (ZnO-JCPDS No. 36-1451 and Dy_2O_3 – JCPDS 01-079-1722) [23]. The hump observed around 2θ value of 10-20º confirmed the presence of silica in the prepared DLCS nanomaterial.

UV-DRS and FESEM of DLCS

The DLCS nanomaterial was analysed by UV-DRS and FESEM analysis and the results are shown in Fig. 2. The absorption spectrum of DLCS showed the onset of absorption peaks in 200–400 nm range and the nanomaterial would also be active in the visible region (Fig. 2A). The band gap energy was found to be 2.82 eV by drawing a plot of Ahv^2 *vs*. hv. The FESEM image of the prepared DLCS is shown in Fig. 2B, the particles were found to have cauliflower like morphology with particles sizes ranging from 40-60 nm.

Photocatalytic degradation of OG and MG dyes

Preliminary studies

The preliminary studies such as effect of dopant concentration, initial pH, dosage of catalyst and dye concentration were conducted under visible light irradiation. The results are shown in Fig. 3. The effect of ZnO loading on DS core shell for 10 mg catalyst/ 10 mL of 10 ppm dye were conducted. It was observed that as the concentration of ZnO on DS core shell increased, the percentage of degradation increased till 1:3 ratio (DLCS3) and then decreased for 1:4 ratio (DLSC4). It increased from 20.63% to 71% for OG dye and 41.89 to 85.97% for MG for DLCS3 photocatalyst. Hence DLCS3 was fixed as the best ratio and further studies were conducted with DLCS3, (Fig. 3A). The effect of aqueous phase pH was studied in a pH range of 2.88 to 11.75 (10 mg/ 10 mL of 10 ppm dyes). It showed maximum percentage of degradation at pH 6.45 (74.98% (OG) and 88.23%

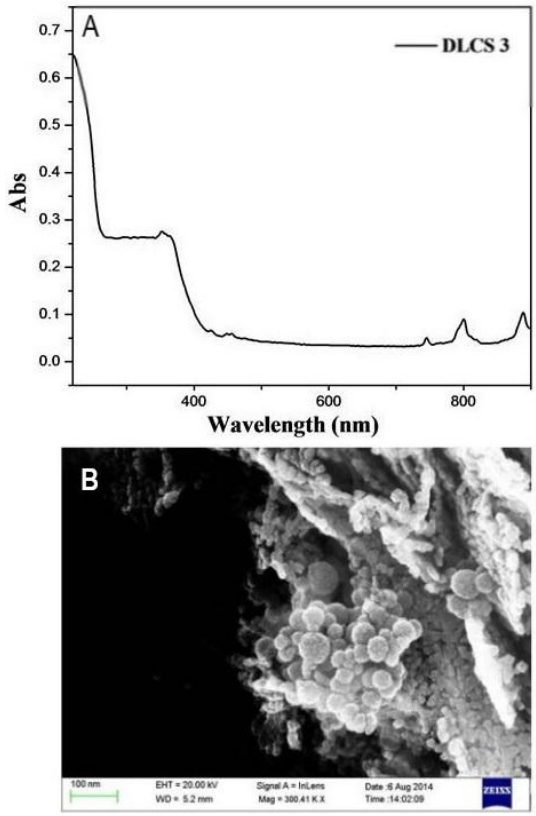

Fig. 2 — (A) UV-DRS spectrum and (B) FESEM image of prepared DLCS nanomaterials

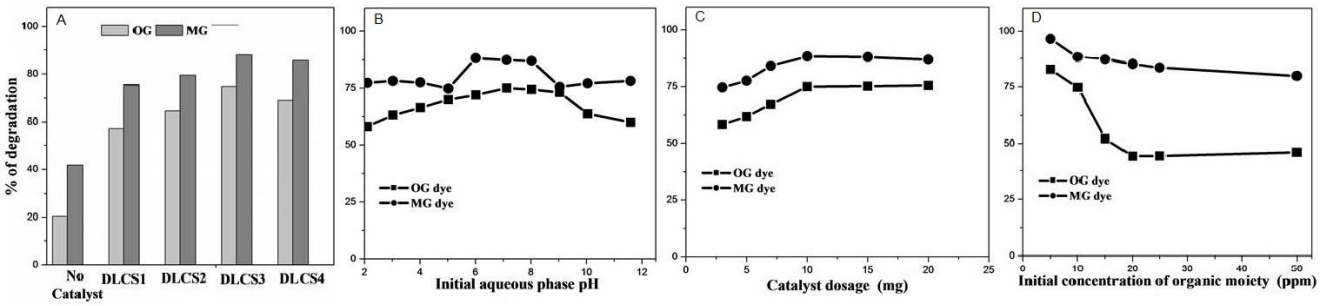

Fig. 3 — Plots for the effect of (A) dopant concentration, (B) initial pH, (C) dosage of catalyst and (D) 2,4-D concentration under visible light irradiation

(MG), (Fig. 3B). The effect of catalyst dosage was conducted from 3 mg to 20 mg/10 mL (10 mL of 10 ppm dyes at pH 6.45). As the amount of catalyst dosage increased from 3 to 10 mg, the percentage degradation increased from 58.3% to 74.98% for OG and 74.62% to 88.37% for MG dye, respectively. After that upon increasing the dosage of the catalyst, the percentage of degradation marginally decreased. The reason may be attributed to the fact that, as the catalyst dosage is increased above 10 mg, the concentration of catalyst is very high which prevent the penetration of photons thereby decreasing the production of OH radicals. Hence 10 mg/10 mL was fixed as the optimum catalyst dosage (Fig. 3C). Studies on the effect of concentration of OG and MG were conducted from 5 to 50 ppm (10 mg/10 mL at pH 6.45). As the concentration of OG and MG dyes in solution increased, the degradation decreased from 82.78%-OG and 96.59%-MG (5 ppm) to 46.19%-OG and 79.81%-MG (50 ppm), respectively (Fig. 3D).

Kinetic studies and COD analysis

The studies on the increase in percentage of degradation with respect to time were conducted for 10, 15, 20 and 25 ppm of OG and MG in 200 mL of dye solution at pH 6.45 with a catalyst dosage of 200 mg. During the course of the reaction, aliquots of sample were collected, centrifuged and analysed by UV-visible absorbance measurement. The results are shown in Fig. 4. The percentage of degradation reached more than 99% in 600, 720, 1020, 1380 min for OG dye and 40, 60, 80 and 100 min for MG dye for the corresponding 10, 15, 20 and 25 ppm, respectively (Figs. 4 A & B). The kinetics of the photocatalytic degradation followed a pseudo-first order and the rate constants were found to be 6.07, 5.43, 3.64 and 2.13 X 10^{-3} min^{-1} (OG) and 77.82, 49.24, 40.28 and 34.01 min^{-1} (MG) for 10, 15, 20 and 25 ppm of the corresponding dyes respectively (Figs 4 B & C). Figs. 4E & 4F show the decrease in COD of the degraded OG and MG solutions and the COD decreased for 10 ppm of OG and MG dyes from 567.36 to 15.76 mg/L and 488.56 to 15.76 mg/L respectively. Since the COD is less than 16 mg/L for even 25 ppm proves that the prepared photocatalyst was effectively degrading the azo and non-azo dyes.

Effect of electrolytes

Studies on the effect of electrolytes were conducted to test the efficacy of the prepared photocatalyst for degrading the selected OG and MG dyes under different environmental conditions (Fig. 5). Since, wastewater may contain different kinds of electrolytes, the prepared photocatalyst is said to be

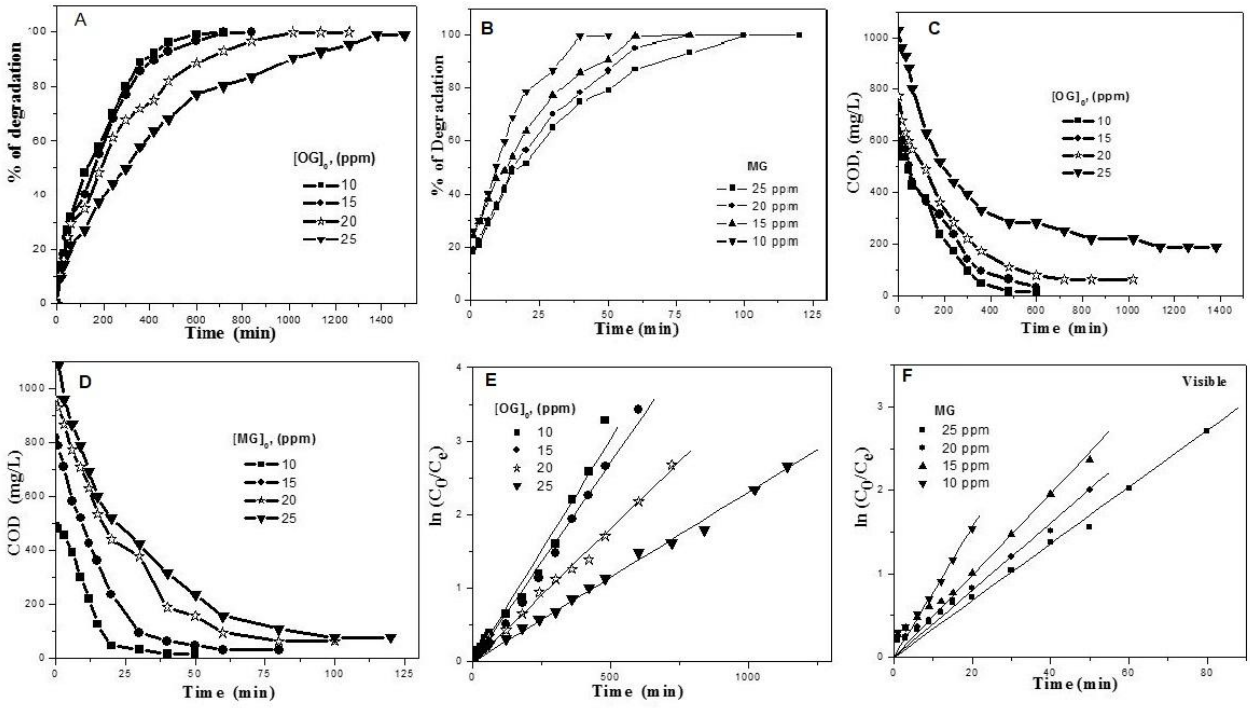

Fig. 4 — Plot on (A and B) percentage degradation w.r.t time, (C and D) plots for pseudo-first order kinetics and (E and F) COD of dye dedgradation using DLCS3 under visible light irradiation

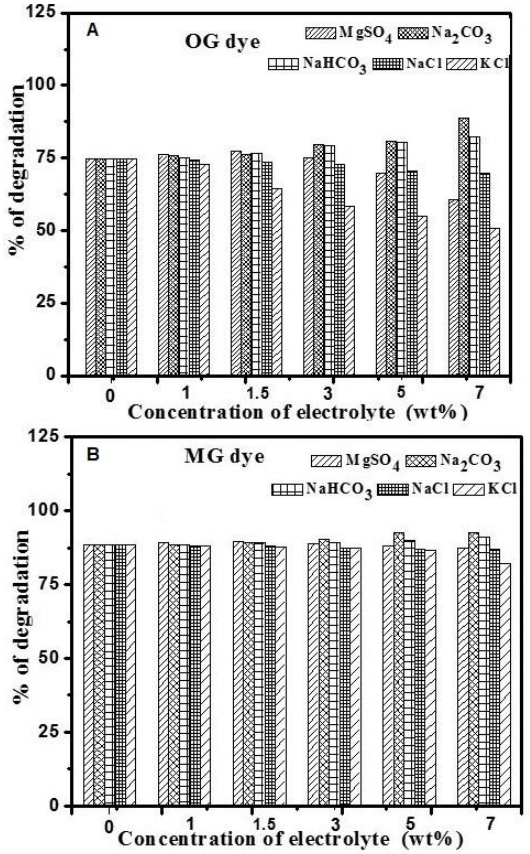

Fig. 5 — Effect of electrolytes on the degradation of OG and MG by DLCS3 photocatalyst

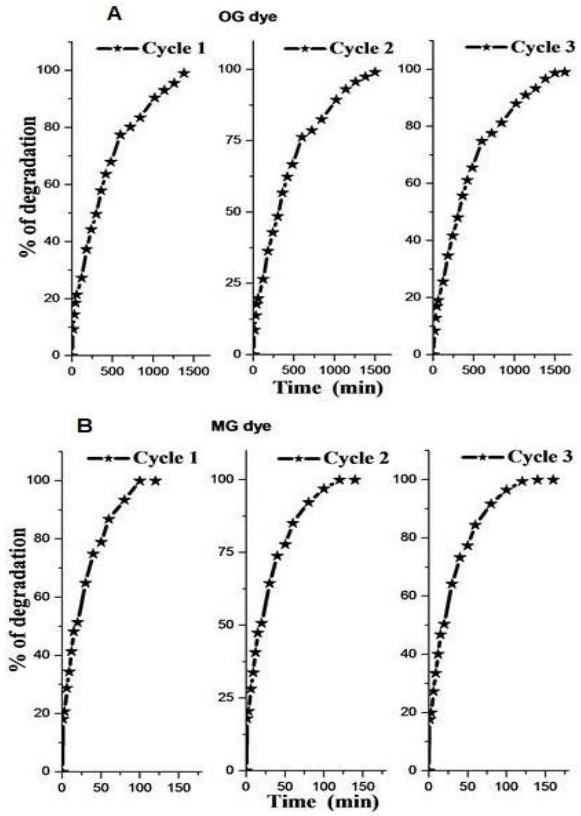

Fig. 6 — Plots for recyclability studies on the degradation of OG and MG by DLCS3 photocatalyst

efficient only if it works in different environments. Electrolytes such as KCl, NaCl, $MgSO_4$, Na_2CO_3 and $NaHCO_3$ were used for evaluation and the concentration varied from 1 to 7% (wt %) for 10 mL of 10 ppm OG, MG (10 mg DLCS3). It has been noticed that the presence of chlorides and sulphates decreased the percentage of degradation as they compete the adsorption of dyes on the catalyst surface.[24] Whereas, Na_2CO_3 and $NaHCO_3$ increased the percentage of degradation as the concentration of electrolyte increased.[25] Compared to OG dye, MG dye showed only marginal to no decrease in activity. This proves that the prepared photocatalyst is effective even in the presence of the tested electrolytes.

Reusability of the prepared NMRO4 photocatalyst

Reusability is an economical factor, because usage of the same catalyst for a number of cycles reduces the cost of the process on the whole. Reusability tests were conducted for the prepared DLCS3 for 3 cycles of operation and the results are shown in Fig. 6. The degradation percentage of the OG and MG molecules were between 97 to 99% even up to three cycles of operation. It was observed that the prepared photocatalyst was very active even in the third cycle of usage.

Conclusions

In the present study, a double layered core-shell material (DLCS) was prepared by a template mediated technique, characterized and photocatalytic activities were conducted for the degradation of OG and MG dyes under visible light irradiations. A comparative study was conducted which showed that the photodegradation was in the order of MG > OG under visible irradiations. The time taken for the complete degradation was recorded as 600 and 40 min, respectively for the corresponding 10 ppm dye solutions, respectively. Hence, it is concluded that non-azo dyes were degraded in lesser duration than azo-dyes, though the photocatalytic activities were much higher for the prepared DLCS than the pristine nanomaterial. Also, these results open the application of the prepared core shell nanocomposite material as a better photocatalyst for environmental applications under natural solar irradiation.

Conflict of interest

The authors declare no conflict of interests in this study.

References

1 Kusvuran E, Gulnaz O, Samil A & Erbil M, *J Hazard Mater*, 175 (2010) 410.
2 Wang H, Xie C, Zhang W, Cai S, Yang Z & Gui Y, *J Hazard Mater*, 141 (2007) 645.
3 Rao CNR & Cheetham AK, *J Mater Chem*, 11 (2001) 2887.
4 Fenton H J, *J Chem Soc*, 65 (1884) 889.
5 Zaharia C, Suteu D, Muresan A, Muresan R & Popescu A, *Environ Eng Manage J* , 8 (2009) 1359.
6 Suteu D, Zaharia C, Muresan A, Muresan R & Popescu A, *Environ Eng Manage J* , 8 (2009) 1097.
7 Lebedev A, Anariba F, Tan JC, Li X & Wu P, *J Photochem Photobiol A*, 360 (2018) 306.
8 Azizi S, Ahmad M, Mahdavi M & Mohammadi SA, *Bioresour Technol*, 8 (2013) 1841.
9 Murugan E, Geetha Rani DP, Srinivasan K & Muthumary J, *Expert Opin Drug Deliv*, 10 (2013) 1319.
10 Murugan E, Arumugam S & Panneerselvam P, *Int J Polymer Mater*, 65 (2016) 111.
11 Murugan E, Yogaraj V, Rani DPG & Sinha A K, *RSC Adv*, 5 (2015) 106461.
12 Xie W, Li Y, Sun W, Huang J, Xie H & Zhao X, *J Photochem Photobiol A*, 216 (2010) 149.
13 Helali S, Polo-López MI, Fernández-Ibáñez P, Ohtani B, Amano F, Malato S & Guillard C, *J Photochem Photobiol A*, 276 (2014) 31.
14 Zhang Q, Zhao X, Duan L, Shen H & Liu R, *J Photochem Photobiol A*, 392 (2020) 112156.
15 Brown MA & De Vito SC, *Environ Sci Technol*, 23 (1993) 249.
16 Robinson T, McMullan G, Marchant R & Nigam P, *Bioresour Technol*, 77 (2001) 247.
17 Soloman PA, Basha CA, Ramamurthi V, Koteeswaran K & Balasubramanian N, *Clean Soil Air Water*, 37 (2009) 889.
18 Saini RD, *Int J Comput Eng Res*, 9 (2017) 121.
19 Chen S, Zhang J, Zhang C, Yue Q, Li Y & Li C, *Desalination*, 252 (2010) 149.
20 Dulman V, Maria Cucu-Man S, Olariu R I, Buhaceanu R, Dumitras M & Bunia I, *Dyes Pigments*, 95 (2012) 79.
21 Clemmensen S, Jensen JC, Jensen N J, Meyer O, Olsen P & Würtzen G, *Arch Toxicol*, 56 (1984) 43.
22 Suganya Josephine GA & Sivasamy A, *ACS Omega*, 3 (2018) 1090.
23 Hong RY, Li J H, Chen LL, Liu Q, Li HZ, Zheng Y & Ding J, *Powder Technol*, 189 (2009) 426.
24 Zhang Y, Zhang KL, Jia MK, Tang H, Sun JT & Yuan L, *J Chin Chem Lett*, 13 (2002) 587.
25 Sahu S & Mohapatra S, *Dalton Trans*, 42 (2013) 2224.
26 Suganya Josephine GA & Sivasamy A, *Appl Catal B*, 150-151 (2014) 288.
27 Peralta-Zamora P, Gouvea CAK, Wypych F & Duran N, *Toxicol Environ Chem*, 80 (2001) 83.
28 Trabelsi H, Atheba P, Gbassi GK, Ksibi M & Drogui P, *Int J Hazard Mater*, 1 (2012) 6.